

Supporting Information for

Human cerebellum and corticocerebellar connections involved in emotional memory enhancement

Matthias Fastenrath^{1,2}, Klara Spalek^{1,2,3}, David Coynel^{1,2}, Eva Loos^{1,2}, Annette Milnik^{2,3}, Tobias Egli^{2,3}, Nathalie Schicktzanz^{1,2}, Léonie Geissmann^{1,2}, Benno Roozendaal⁴, Andreas Papassotiropoulos^{2,3,5,6}, Dominique J F de Quervain^{1,2,5}

¹Division of Cognitive Neuroscience, Faculty of Medicine, University of Basel, Switzerland

²Research Platform Molecular and Cognitive Neurosciences, University of Basel, Switzerland

³Division of Molecular Neuroscience, Faculty of Medicine, University of Basel, Switzerland

⁴Department of Cognitive Neuroscience, Radboud university medical center, and Donders Institute for Brain, Cognition and Behaviour, Radboud University, Nijmegen, The Netherlands

⁵Psychiatric University Clinics, University of Basel, Switzerland

⁶Department Biozentrum, Life Sciences Training Facility, University of Basel, Switzerland

Correspondence: Dominique J F de Quervain: Email: dominique.dequervain@unibas.ch

This PDF file includes:

Tables S1 to S9
Figures S1 to S10

DCM model (R12 and one other ROI)	Sample size in discovery sample	Sample size in replication sample
R1 and R12	901	433
R2 and R12	899	429
R3 and R12	899	429
R4 and R12	862	419
R5 and R12	852	411
R6 and R12	894	422
R8 and R12	881	426
R9 and R12	798	378
R10 and R12	899	432
R14 and R12	902	432
R15 and R12	837	410
R16 and R12	902	433
R17 and R12	899	432
R18 and R12	902	432
R19 and R12	901	433
R20 and R12	902	433
R21 and R12	902	433
R22 and R12	902	433
R23 and R12	902	433
R24 and R12	901	433
R26 and R12	902	433
R27 and R12	902	433
R28 and R12	902	433
R29 and R12	902	433
R30 and R12	899	432

Table S1. Number of subjects per DCM between replicating ROIs. The table lists the sample size after the exclusion of subjects from whom time courses could not be successfully extracted. Sample size without exclusions due to unsuccessful time course extraction: Discovery sample N = 945; replication sample N = 473. Table refers to Materials and Methods, paragraph “*Time course extraction from ROIs*”. R: ROI

ROI	Percentage of excluded subjects in discovery sample	Percentage of excluded subjects in replication sample
1	0.11%	0%
2	0.42%	0.85%
3	0.42%	0.85%
4	4.87%	3.59%
5	5.92%	5.29%
6	1.27%	2.54%
8	2.54%	1.69%
9	11.64%	14.16%
10	0.32%	0.21%
12	4.55%	8.46%
14	0%	0.21%
15	7.20%	5.92%
16	0%	0%
17	0.32%	0.21%
18	0%	0.21%
19	0.11%	0%
20	0%	0%
21	0%	0%
22	0%	0%
23	0%	0%
24	0.11%	0%
26	0%	0%
27	0%	0%
28	0%	0%
29	0%	0%
30	0.32%	0.21%

Table S2. Percentage of subjects per replicating ROI that had to be excluded as they did not show robust activation (Table refers to Materials and Methods, paragraph “*Time course extraction from ROIs*”).

ROI from parcellation	Maximum t value within ROI	Regional correspondence of the local maxima within ROI	MNI coordinates at maximum		
			X	Y	Z
1	12.0263	ctx-lh-inferiorparietal (1%) ctx-lh-inferiortemporal (11%) ctx-lh-lateraloccipital (54%) ctx-lh-middletemporal (5%)	-49.5	-74.25	0
2	7.0601	ctx-lh-postcentral (3%) ctx-lh-supramarginal (80%)	-63.25	-27.5	28
3	8.6389	ctx-lh-fusiform (36%) ctx-lh-inferiortemporal (33%)	-44	-46.75	-20
4	7.2131	ctx-rh-superiorparietal (59%)	16.5	-85.25	40
5	6.6197	ctx-rh-postcentral (8%) ctx-rh-supramarginal (30%)	66	-16.5	40
6	6.6173	ctx-lh-lateraloccipital (1%) ctx-lh-superiorparietal (29%)	-19.25	-85.25	32
7	6.3562	ctx-lh-posteriorcingulate (56%) ctx-rh-posteriorcingulate (14%)	0	0	36
8	7.1087	ctx-rh-superiorparietal (59%)	27.5	-55	64
9	6.4531	ctx-rh-caudalmiddlefrontal (4%) ctx-rh-precentral (50%)	46.75	0	56
10	7.5141	ctx-lh-precuneus (1%) ctx-rh-cuneus (10%) ctx-rh-lingual (23%) ctx-rh-pericalcarine (5%) ctx-rh-precuneus (2%)	2.75	-63.25	12
12	5.7674	Right-Cerebellum-Cortex (1%) Left-Cerebellum-Cortex (97%) Vermis IX (76%), Left IX (14%) ¹	-2.75	-55	-40
13	6.3208	ctx-lh-superiorparietal (26%)	-30.25	-55	68
14	7.6908	Left-Pallidum (5%) Left-VentralDC (15%)	-8.25	-5.5	-8
15	5.9768	ctx-rh-middletemporal (56%)	57.75	-8.25	-20
16	8.3868	ctx-lh-lingual (3%) ctx-lh-pericalcarine (46%)	-13.75	-74.25	8
17	8.3571	ctx-lh-insula (6%)	-33	0	-20
18	10.9539	ctx-rh-fusiform (10%) ctx-rh-inferiortemporal (20%) ctx-rh-lateraloccipital (19%) ctx-rh-middletemporal (1%)	46.75	-63.25	-8
19	7.4373	ctx-lh-lateralorbitofrontal (21%) ctx-lh-insula (54%)	-30.25	13.75	-16
20	8.8163	ctx-lh-isthmuscingulate (55%) ctx-lh-precuneus (17%)	-5.5	-49.5	28
21	8.527	Brain-Stem (24%) Right-VentralDC (61%)	13.75	-22	-12
22	10.537	ctx-lh-medialorbitofrontal (3%) ctx-lh-rostralanteriorcingulate (68%) ctx-lh-superiorfrontal (10%)	-2.75	44	0
23	11.869	ctx-rh-inferiortemporal (23%) ctx-rh-lateraloccipital (35%) ctx-rh-middletemporal (8%)	52.25	-66	-4
24	8.3787	ctx-rh-lateralorbitofrontal (67%) ctx-rh-insula (12%)	30.25	16.5	-20
25	7.9919	ctx-rh-insula (90%)	35.75	11	-12

26	9.1318	Right-Amygdala (98%)	19.25	-5.5	-16
27	10.1738	ctx-lh-medialorbitofrontal (6%) ctx-lh-rostralanteriorcingulate (10%) ctx-lh-superiorfrontal (51%)	-2.75	52.25	4
28	10.7336	ctx-lh-inferiorparietal (4%) ctx-lh-inferiortemporal (16%) ctx-lh-lateraloccipital (13%) ctx-lh-middletemporal (37%)	-52.25	-68.75	4
29	10.4155	ctx-rh-inferiorparietal (2%) ctx-rh-inferiortemporal (18%) ctx-rh-lateraloccipital (10%) ctx-rh-middletemporal (34%)	52.25	-60.5	0
30	9.0748	ctx-lh-caudalanteriorcingulate (6%) ctx-rh-caudalanteriorcingulate (29%) ctx-rh-corpuscallosum (1%) CC_Anterior (3%)	2.75	27.5	16

Table S3. Increased activity during successful emotional memory encoding in the discovery sample (N = 944). Table shows the local maxima per region of interest (ROI). Regions are in accordance to FreeSurfer nomenclature. Percentages denote the share of participants with a certain label located at a given coordinate (see Materials and Methods, paragraph “Anatomical localization of ROIs based on a population-averaged anatomical probabilistic atlas”).¹ Assignment based on FSL atlas “Cerebellar Atlas in MNI152 space after normalization with FNIRT” (Diedrichsen et al., 2009).

ROI from parcellation	Maximum t value within ROI	Regional correspondence of the local maxima within ROI	MNI coordinates at maximum		
			X	Y	Z
1	8.3442	ctx-lh-fusiform (4%) ctx-lh-inferiortemporal (12%) ctx-lh-lateraloccipital (43%) ctx-lh-middletemporal (1%)	-46.75	-71.5	-4
2	4.9721	ctx-lh-supramarginal (55%)	-55	-35.75	28
3	6.9116	ctx-lh-fusiform (47%) ctx-lh-inferiortemporal (16%) ctx-lh-lateraloccipital (7%)	-44	-63.25	-12
4	6.1305	ctx-rh-superiorparietal (56%)	22	-85.25	44
5	4.6385	ctx-rh-postcentral (2%) ctx-rh-supramarginal (24%)	66	-19.25	44
6	4.9083	ctx-lh-inferiorparietal (3%) ctx-lh-superiorparietal (67%)	-19.25	-85.25	40
7	4.285 †	ctx-lh-posteriorcingulate (56%) ctx-rh-posteriorcingulate (14%)	0	0	36
8	4.4662	ctx-rh-superiorparietal (46%)	33	-52.25	68
9	5.4453	ctx-rh-caudalmiddlefrontal (4%) ctx-rh-precentral (70%)	49.5	2.75	48
10	5.2734	ctx-rh-lingual (43%)	8.25	-60.5	4
12	5.122	Right-Cerebellum-Cortex (93%) Left-Cerebellum-Cortex (6%) Right IX (75%), Vermis IX (22%), Vermis VIIIb (2%) ¹	2.75	-57.75	-44
13 †	3.5337	ctx-lh-superiorparietal (43%)	-30.25	-49.5	60
14	6.2463	Left-Pallidum (1%) Left-Amygdala (6%) Left-VentralDC (49%)	-13.75	-5.5	-12

15	5.626	ctx-rh-middletemporal (68%) ctx-rh-superiortemporal (2%)	55	-8.25	-20
16	6.1707	ctx-lh-cuneus (2%) ctx-lh-lingual (1%) ctx-lh-pericalcarine (54%)	-8.25	-74.25	12
17	8.051	Left-Amygdala (92%)	-19.25	-5.5	-16
18	8.1444	ctx-rh-fusiform (10%) ctx-rh-inferiortemporal (20%) ctx-rh-lateraloccipital (19%) ctx-rh-middletemporal (1%)	46.75	-63.25	-8
19	5.5845	ctx-lh-lateralorbitofrontal (64%) ctx-lh-insula (11%)	-30.25	16.5	-16
20	6.8923	ctx-lh-isthmuscingulate (7%) ctx-lh-precuneus (39%) ctx-rh-precuneus (10%)	0	-55	28
21	5.406	Brain-Stem (95%)	5.5	-30.25	-4
22	7.362	ctx-lh-medialorbitofrontal (1%) ctx-lh-rostralanteriorcingulate (52%) ctx-lh-superiorfrontal (27%)	-2.75	46.75	4
23	8.8366	ctx-rh-fusiform (5%) ctx-rh-inferiortemporal (19%) ctx-rh-lateraloccipital (34%) ctx-rh-middletemporal (2%)	49.5	-66	-8
24	5.6773	ctx-rh-lateralorbitofrontal (22%) ctx-rh-insula (50%)	27.5	13.75	-16
25	3.8598 †	ctx-rh-lateralorbitofrontal (5%) ctx-rh-parsorbitalis (40%) ctx-rh-parstriangularis (17%)	46.75	27.5	-8
26	6.836	Right-Hippocampus (1%) Right-Amygdala (85%) Right-VentralDC (6%)	16.5	-5.5	-16
27	7.1583	ctx-lh-rostralanteriorcingulate (25%) ctx-lh-superiorfrontal (49%)	-2.75	49.5	8
28	7.7959	ctx-lh-inferiorparietal (4%) ctx-lh-inferiortemporal (16%) ctx-lh-lateraloccipital (13%) ctx-lh-middletemporal (37%)	-52.25	-68.75	4
29	7.4797	ctx-rh-inferiortemporal (27%) ctx-rh-lateraloccipital (8%) ctx-rh-middletemporal (21%)	55	-60.5	-4
30	6.0532	ctx-lh-caudalanteriorcingulate (42%) ctx-lh-corporuscallosum (2%) ctx-rh-caudalanteriorcingulate (2%) CC_Anterior (4%)	0	27.5	16

Table S4: Increased activity during successful emotional memory encoding in the replication sample (N = 470). Table shows the local maxima per region of interest (ROI). Regions are in accordance to FreeSurfer nomenclature. Percentages per coordinate denote the population-average probability of an anatomical label (see Materials and Methods, paragraph “Anatomical localization of ROIs based on a population-averaged anatomical probabilistic atlas”). ¹ Assignment based on FSL atlas “Cerebellar Atlas in MNI152 space after normalization with FNIRT” (Diedrichsen et al., 2009). † Maxima for clusters 7, 13 and 25 did not reach significance threshold ($T = 4.4056$, $P < 0.05$, one-sided, Bonferroni corrected for 7635 tests).

ROI from parcellation	Size of ROI	Anatomical correspondence of centroid [MNI]	Anatomical regions spanned by ROI	Average percentage regional correspondence
1	462	ctx-lh-lateraloccipital (53%) Left-Cerebral-White-Matter (36%) [-44 -77 0]	ctx-lh-fusiform	6.9
			ctx-lh-inferiortemporal	5.97
			ctx-lh-lateraloccipital	32.34
			Left-Cerebral-White-Matter	24.08
			ctx-lh-middletemporal	2.26
			ctx-lh-inferiorparietal	5.07
2	232	ctx-lh-postcentral (4%) ctx-lh-supramarginal (59%) Left-Cerebral-White-Matter (31%) [-60.5 -27.5 32]	ctx-lh-supramarginal	44.83
			ctx-lh-postcentral	8.46
			Left-Cerebral-White-Matter	14.25
3	181	ctx-lh-fusiform (59%) ctx-lh-inferiortemporal (10%) Left-Cerebral-White-Matter (22%) [-41.25 -52.25 -16]	Left-Cerebellum-Cortex	8.81
			ctx-lh-fusiform	32.74
			ctx-lh-inferiortemporal	24.09
			Left-Cerebral-White-Matter	21.1
4	127	ctx-rh-superiorparietal (42%) Right-Cerebral-White-Matter (53%) [19.25 -85.25 36]	Right-Cerebral-White-Matter	31.58
			ctx-rh-lateraloccipital	2.64
			ctx-rh-superiorparietal	39.21
5	101	ctx-rh-postcentral (1%) ctx-rh-supramarginal (64%) Right-Cerebral-White-Matter (31%) [63.25 -24.75 32]	Right-Cerebral-White-Matter	13.24
			ctx-rh-superiortemporal	1.21
			ctx-rh-supramarginal	50.59
			ctx-rh-postcentral	5.88
6	141	ctx-lh-superiorparietal (24%) Left-Cerebral-White-Matter (72%) [-16.5 -85.25 32]	Left-Cerebral-White-Matter	38.86
			ctx-lh-inferiorparietal	1.41
			ctx-lh-lateraloccipital	4.54
			ctx-lh-superiorparietal	34.41
			ctx-lh-cuneus	3.36
7	66	ctx-lh-posteriorcingulate (61%) Left-Cerebral-White-Matter (3%) ctx-rh-posteriorcingulate (17%) [0 -11 36]	ctx-rh-posteriorcingulate	20.73
			ctx-lh-posteriorcingulate	48.75
			Left-Cerebral-White-Matter	12.27
8	177	ctx-rh-postcentral (1%) ctx-rh-superiorparietal (49%) Right-Cerebral-White-Matter (43%) [30.25 -49.5 64]	Right-Cerebral-White-Matter	18.24
			ctx-rh-superiorparietal	42.09
			ctx-rh-postcentral	1.67
9	76	ctx-rh-caudalmiddlefrontal (4%) ctx-rh-precentral (70%)	Right-Cerebral-White-Matter	10.14
			ctx-rh-caudalmiddlefrontal	5.51

		Right-Cerebral-White-Matter (21%) [49.5 2.75 48]	ctx-rh-precentral	44.31
10	201	ctx-rh-lingual (24%) ctx-rh-pericalcarine (5%) Right-Cerebral-White-Matter (69%) [13.75 -63.25 4]	ctx-rh-lingual	25.07
			Right-Cerebral-White-Matter	39.46
			ctx-rh-pericalcarine	11.13
			ctx-rh-precuneus	3.8
11	60	Left-Caudate (54%) Left-Cerebral-White-Matter (35%) [-16.5 -8.25 24]	ctx-rh-cuneus	3.11
			Left-Cerebellum-Cortex	13.25
			ctx-rh-fusiform	6.52
			Right-Cerebral-White-Matter	8.76
			ctx-lh-middletemporal	3.21
			Left-Cerebral-White-Matter	5.8
			Left-Putamen	1.46
			ctx-lh-superiorfrontal	9.89
12	65	Right-Cerebellum-Cortex (41%) Left-Cerebellum-Cortex (59%) [0 -55 -40]	ctx-lh-precentral	12.19
			ctx-rh-superiorfrontal	7
			Left-Cerebellum-Cortex	38.82
			Left-Cerebellum-White-Matter	3.96
13	110	ctx-lh-postcentral (2%) ctx-lh-superiorparietal (47%) [-33 -46.75 68]	Right-Cerebellum-Cortex	46.53
			Right-Cerebellum-White-Matter	6
			Left-Cerebral-White-Matter	7.16
14	147	Left-Thalamus-Proper (53%) Left-Cerebral-White-Matter (1%) Left-VentralDC (31%) [-2.75 -5.5 -4]	ctx-lh-superiorparietal	32.43
			ctx-lh-postcentral	3.27
			Left-VentralDC	15.25
			Left-Cerebral-White-Matter	19.22
			Left-Pallidum	4.65
			Left-Thalamus-Proper	26.01
			Right-Cerebral-White-Matter	7.01
15	61	ctx-rh-middletemporal (29%) Right-Cerebral-White-Matter (71%) [57.75 -11 -20]	Right-Thalamus-Proper	17.33
			Right-VentralDC	1.64
			Right-Cerebral-White-Matter	40.22
16	354	ctx-lh-cuneus (4%) ctx-lh-lingual (22%) ctx-lh-pericalcarine (33%)	ctx-rh-superiortemporal	5.74
			Left-Cerebellum-Cortex	2.69
			ctx-lh-lingual	18.92
			Left-Cerebral-White-Matter	36.72

		Left-Cerebral-White-Matter (18%) [-8.25 -68.75 8]	ctx-lh-pericalcarine	10.09
			ctx-lh-precuneus	5.69
			ctx-lh-cuneus	7.68
17	205	Left-Amygdala (54%) [-27.5 -2.75 -20]	Left-Cerebral-White-Matter	25.56
			ctx-lh-temporalpole	1.06
			Left-Amygdala	19.39
			ctx-lh-superiortemporal	3.57
			Left-Hippocampus	1.93
			ctx-lh-insula	7.44
			Left-Putamen	1.12
18	261	ctx-rh-fusiform (53%) ctx-rh-inferiortemporal (10%) ctx-rh-lateraloccipital (2%) Right-Cerebral-White-Matter (30%) [44 -55 -16]	Right-Cerebellum-Cortex	9.77
			ctx-rh-fusiform	33.55
			ctx-rh-inferiortemporal	14.49
			Right-Cerebral-White-Matter	27.58
			ctx-rh-lateraloccipital	3.35
19	210	ctx-lh-lateralorbitofrontal (13%) ctx-lh-superiortemporal (6%) [-35.75 13.75 -20]	Left-Cerebral-White-Matter	7.79
			ctx-lh-middletemporal	3.71
			ctx-lh-superiortemporal	11.93
			ctx-lh-temporalpole	3.69
			ctx-lh-lateralorbitofrontal	20.11
20	348	ctx-lh-isthmuscingulate (44%) ctx-lh-precuneus (38%) Left-Cerebral-White-Matter (3%) [-2.75 -52.25 28]	ctx-rh-precuneus	13.26
			ctx-lh-isthmuscingulate	14.17
			ctx-lh-precuneus	24.89
			Left-Cerebral-White-Matter	16.85
			ctx-rh-isthmuscingulate	7.93
			Right-Cerebral-White-Matter	3.49
21	303	Brain-Stem (95%) Left-VentralDC (5%) [-2.75 -27.5 -12]	Brain-Stem	39.72
			Right-VentralDC	10.37
			Left-VentralDC	19.28
			Left-Cerebral-White-Matter	2.76
			Left-Hippocampus	4.83
			Left-Thalamus-Proper	4.21
			Right-Thalamus-Proper	1.17
22	604	ctx-lh-rostralanteriorcingulate (45%) ctx-lh-superiorfrontal (2%)	Left-Cerebral-White-Matter	13.67
			ctx-lh-medialorbitofrontal	6.44
			ctx-lh-rostralanteriorcingulate	14.73

		ctx-rh-rostralanteriorcingulate (11%) [0 41.25 4]	ctx-rh-rostralanteriorcingulate	10.75
			ctx-rh-medialorbitofrontal	4.24
			Right-Cerebral-White-Matter	7.11
			ctx-rh-superiorfrontal	6.67
			ctx-lh-superiorfrontal	9.46
			CC_Anterior	1.3
			ctx-rh-caudalanteriorcingulate	3.06
			ctx-lh-caudalanteriorcingulate	3.48
23	487	ctx-rh-inferiorparietal (3%) ctx-rh-inferiortemporal (3%) ctx-rh-lateraloccipital (56%) Right-Cerebral-White-Matter (26%) [46.75 -71.5 0]	ctx-rh-lateraloccipital	32.03
			ctx-rh-fusiform	3.3
			Right-Cerebral-White-Matter	29.37
			ctx-rh-inferiortemporal	4.77
			ctx-rh-middletemporal	3.28
			ctx-rh-inferiorparietal	12.83
24	259	ctx-rh-superiortemporal (44%) ctx-rh-temporalpole (31%) [35.75 16.5 -28]	ctx-rh-temporalpole	8.46
			ctx-rh-middletemporal	6.76
			ctx-rh-superiortemporal	15.08
			Right-Cerebral-White-Matter	10.79
			ctx-rh-lateralorbitofrontal	19.56
			ctx-rh-insula	5.51
25	232	ctx-rh-parsorbitalis (1%) ctx-rh-insula (47%) [44 16.5 -8]	ctx-rh-insula	27.66
			ctx-rh-superiortemporal	6.7
			Right-Cerebral-White-Matter	13.36
			ctx-rh-lateralorbitofrontal	2.13
			ctx-rh-parsorbitalis	4.8
			ctx-rh-parstriangularis	11.41
			ctx-rh-parsopercularis	3.76
26	357	Right-Cerebral-White-Matter (1%) Right-Amygdala (74%) [22 -2.75 -16]	Right-Cerebral-White-Matter	19.26
			Right-Amygdala	13.32
			ctx-rh-lateralorbitofrontal	1.15
			Right-Hippocampus	10.68
			ctx-rh-superiortemporal	1.02
			ctx-rh-insula	4.61
			Right-VentralDC	13.29
			Right-Putamen	4.76
			Right-Accumbens-area	1.7
			Right-Pallidum	3.1
27	654	ctx-lh-superiorfrontal (29%)	ctx-rh-medialorbitofrontal	2.65

		ctx-rh-superiorfrontal (4%) [0 57.75 16]	ctx-lh-medialorbitofrontal	3.18
			Left-Cerebral-White-Matter	9.66
			Right-Cerebral-White-Matter	7.24
			ctx-lh-superiorfrontal	23.64
			ctx-rh-superiorfrontal	21.83
28	503	ctx-lh-bankssts (3%) ctx-lh-inferiorparietal (48%) ctx-lh-lateraloccipital (2%) ctx-lh-middletemporal (11%) ctx-lh-supramarginal (2%) Left-Cerebral-White-Matter (12%) [-49.5 -63.25 16]	Left-Cerebral-White-Matter	25.19
			ctx-lh-inferiortemporal	2.54
			ctx-lh-lateraloccipital	3.39
			ctx-lh-middletemporal	11.21
			ctx-lh-bankssts	4.14
			ctx-lh-inferiorparietal	30.18
			ctx-lh-supramarginal	2.66
29	431	ctx-rh-bankssts (7%) ctx-rh-inferiorparietal (25%) ctx-rh-middletemporal (6%) Right-Cerebral-White-Matter (58%) [55 -52.25 12]	ctx-rh-middletemporal	14.45
			ctx-rh-inferiortemporal	2.45
			ctx-rh-lateraloccipital	1.54
			Right-Cerebral-White-Matter	26.83
			ctx-rh-bankssts	14.3
			ctx-rh-inferiorparietal	23.02
			ctx-rh-supramarginal	3.67
30	220	ctx-lh-caudalanteriorcingulate (55%) Left-Cerebral-White-Matter (1%) ctx-rh-caudalanteriorcingulate (10%) [0 16.5 28]	Right-Cerebral-White-Matter	10.88
			CC_Mid_Anterior	2.79
			CC_Anterior	3.22
			Left-Cerebral-White-Matter	13.16
			ctx-rh-caudalanteriorcingulate	16.86
			ctx-lh-caudalanteriorcingulate	19.71
			ctx-lh-superiorfrontal	2.43
			ctx-rh-posteriorcingulate	3.39
			ctx-lh-posteriorcingulate	5.41

Table S5. Number of voxels and anatomical correspondence per ROI. Percentages per centroid denote the population-average probability of an anatomical label. The average percentage of regional correspondence denotes the proportion of voxels mapping to a specific anatomical region. A 100% correspondence would occur if all voxels of a parcellation would be located within an anatomical region such as the brain stem, and each voxel itself had a probability of 100% of being located in the brain stem. Within a specific voxel, probabilities across anatomical labels do not necessarily sum to 100%, and therefore anatomical correspondence per ROI may not sum to 100%. Regions are in accordance to FreeSurfer nomenclature. The procedure is described in Materials and Methods, paragraph “*Anatomical localization of ROIs based on a population-averaged anatomical probabilistic atlas*”. Regional probabilities smaller than 1% are not shown.

ROI	12
2	0.119
3	0.094
4	0.610
5	0.275
9	0.366
14	0.129
20	0.070
21	0.150
22	0.131
24	0.436
26	0.074
28	0.184
29	0.074
30	0.302

Table S6. Strength of directed connections from the cerebellum (ROI 12) to other ROIs. Table lists connections for the discovery sample. Connection strength as shown in the table represents the change in connection strength during “successful emotional memory encoding” (posterior probability > 0.99).

ROI	3	6	9	10	19	21	22	23	24	28	30
12	0.051	0.110	0.121	0.159	0.152	0.119	0.248	0.041	0.596	0.266	0.160

Table S7. Strength of directed connections from other ROIs to the cerebellum (ROI 12). Table lists connections for the discovery sample. Connection strength as shown in the table represents the change in connection strength during “successful emotional memory encoding” (posterior probability > 0.99).

ROI	12
2	0.256
4	0.188
9	0.778
14	0.155
20	0.128
21	0.284
22	0.060
26	0.650
28	0.093
29	0.118
30	0.091

Table S8. Strength of directed connections from the cerebellum (ROI 12) to other ROIs. Table lists connections for the replication sample. Connection strength as shown in the table represents the change in connection strength during “successful emotional memory encoding” (posterior probability > 0.99).

ROI	9	10	22	23
12	0.355	0.072	0.183	0.253

Table S9. Strength of directed connections from other ROIs to the cerebellum (ROI 12). Table lists connections for the replication sample. Connection strength as shown in the table represents the change in connection strength during “successful emotional memory encoding” (posterior probability > 0.99).

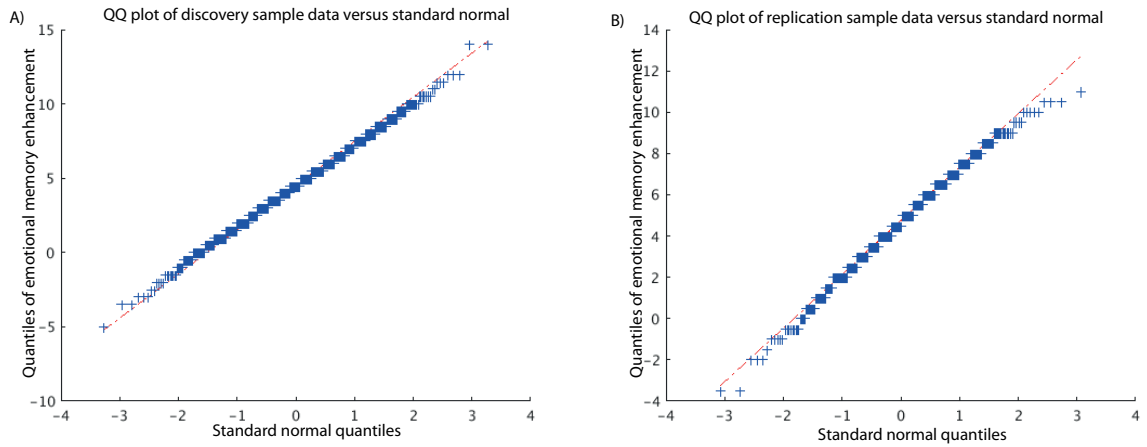


Figure S1. Sample quantiles of the behavioral effect of emotional memory enhancement versus theoretical quantiles from a normal distribution. Panels A and B show results for discovery and replication sample, respectively.

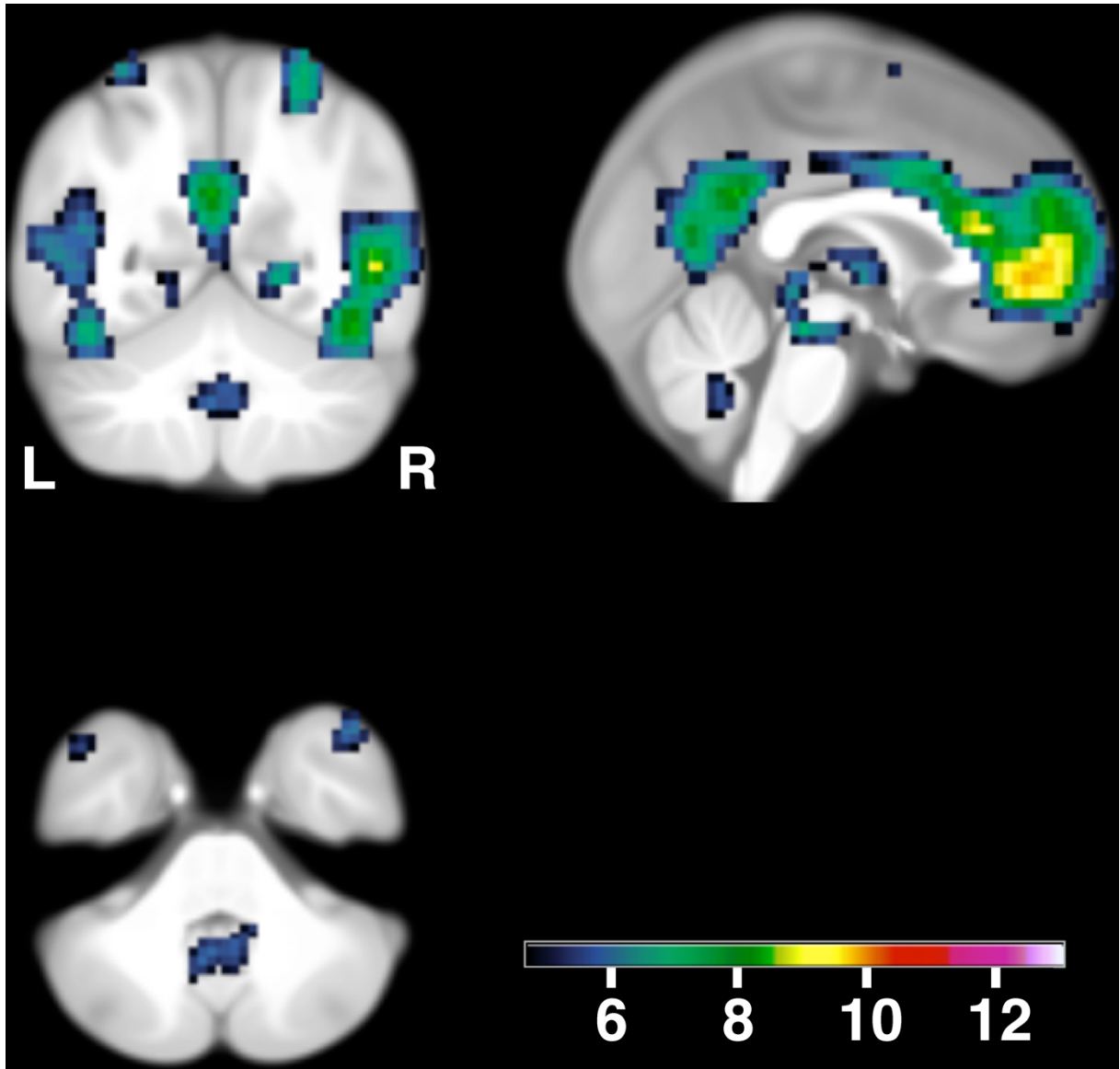


Figure S2. Voxels that show increased activation for successful emotional memory encoding within the discovery sample ($P_{\text{whole-brain-FWE-corrected}} < 0.05$, $N = 944$). Colors code for T-values.

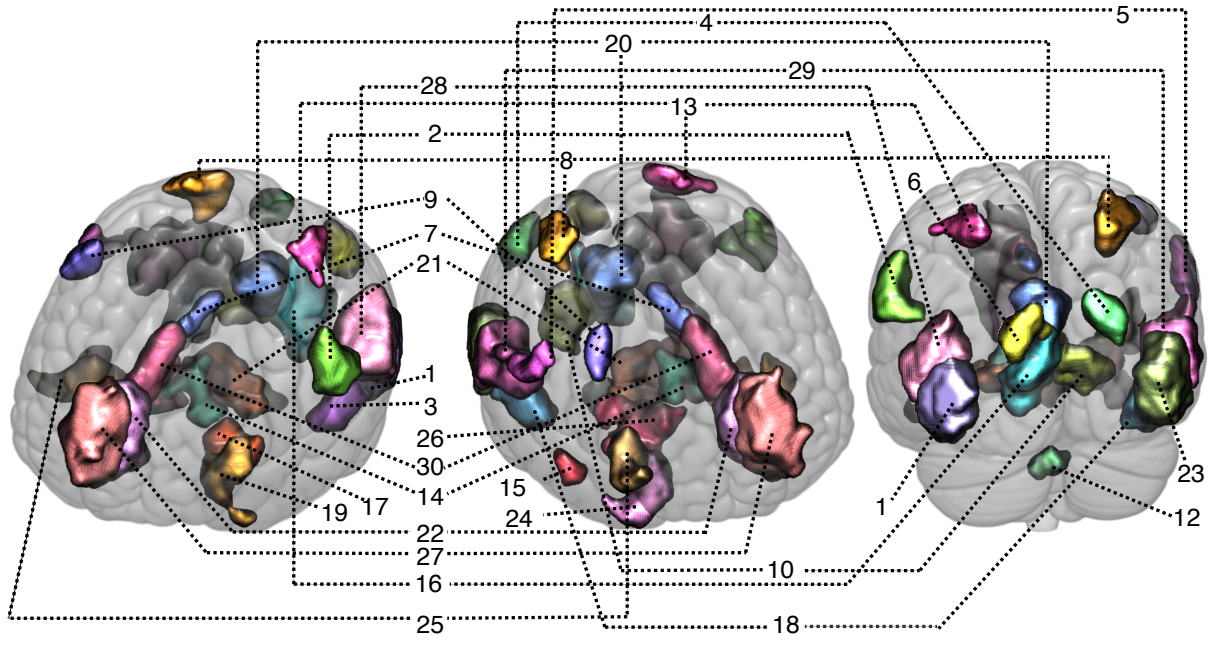


Figure S3. The figure depicts the result of the parcellation, where 29 spatially coherent regions of interest (ROIs) were identified. Different colors denote different ROIs. See Table S5 for anatomical correspondence per ROI.

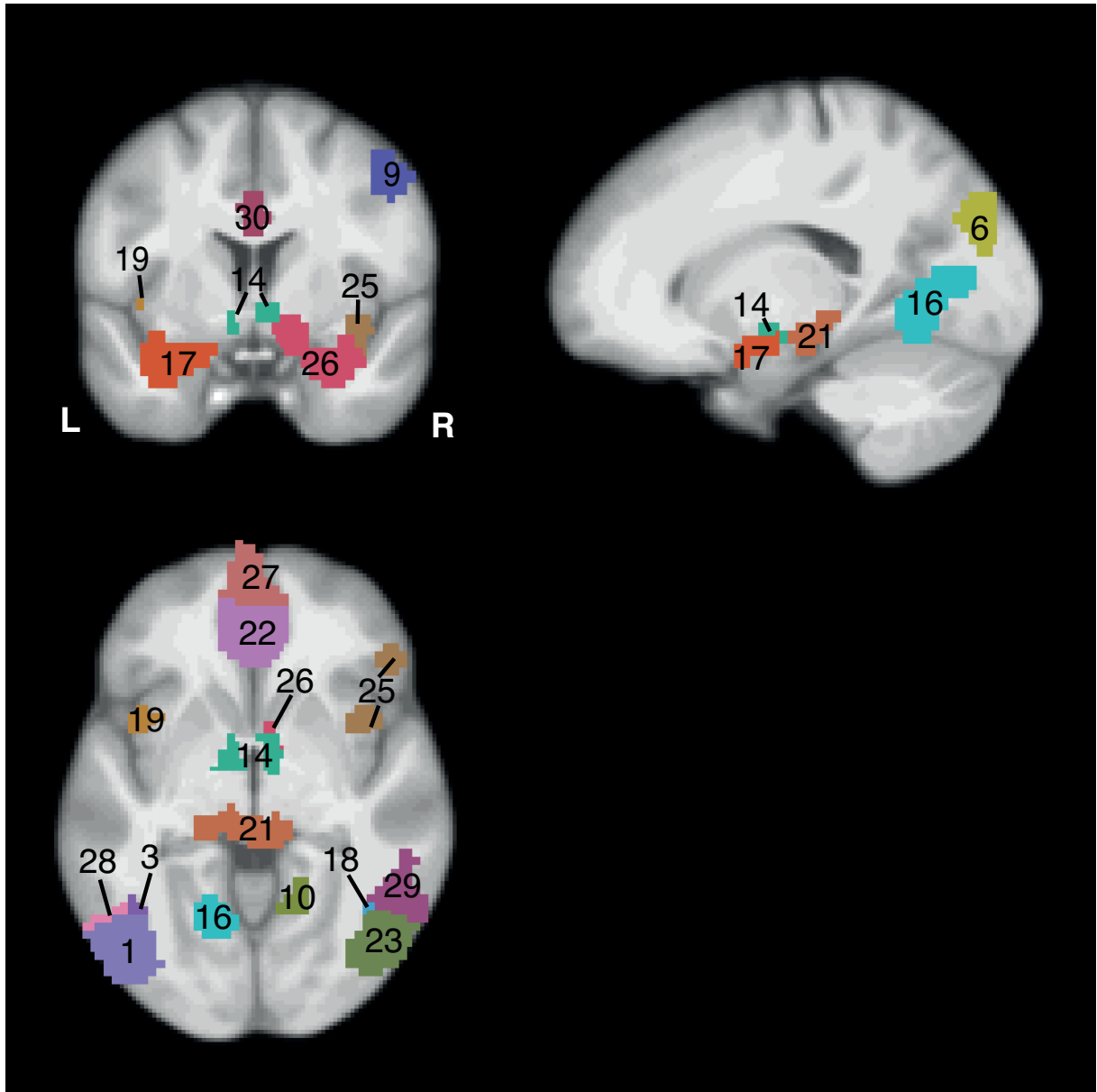


Figure S4. Result of the parcellation, where 29 spatially coherent regions of interest (ROIs) were identified. The figure depicts ROIs: 1, 3, 6, 9, 10, 14, 16, 17, 18, 19, 21, 22, 23, 25, 26, 28, 29, 30. Different colors denote different regions.

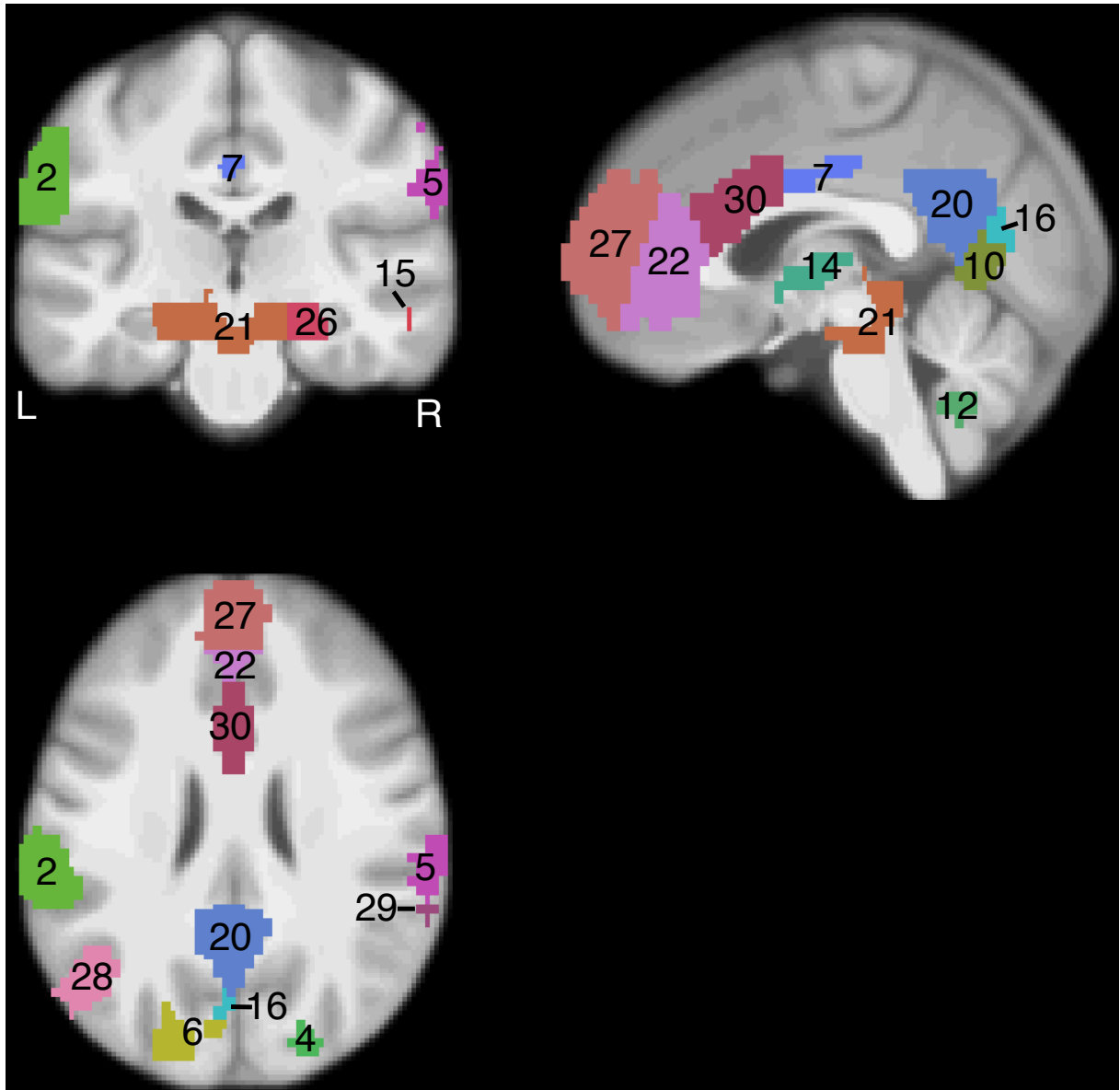


Figure S5. Result of the parcellation, where 29 spatially coherent regions of interest (ROIs) were identified. The figure depicts ROIs: 2, 4, 5, 6, 7, 10, 12, 14, 15, 16, 21, 22, 26, 27, 28, 30. Different colors denote different regions.

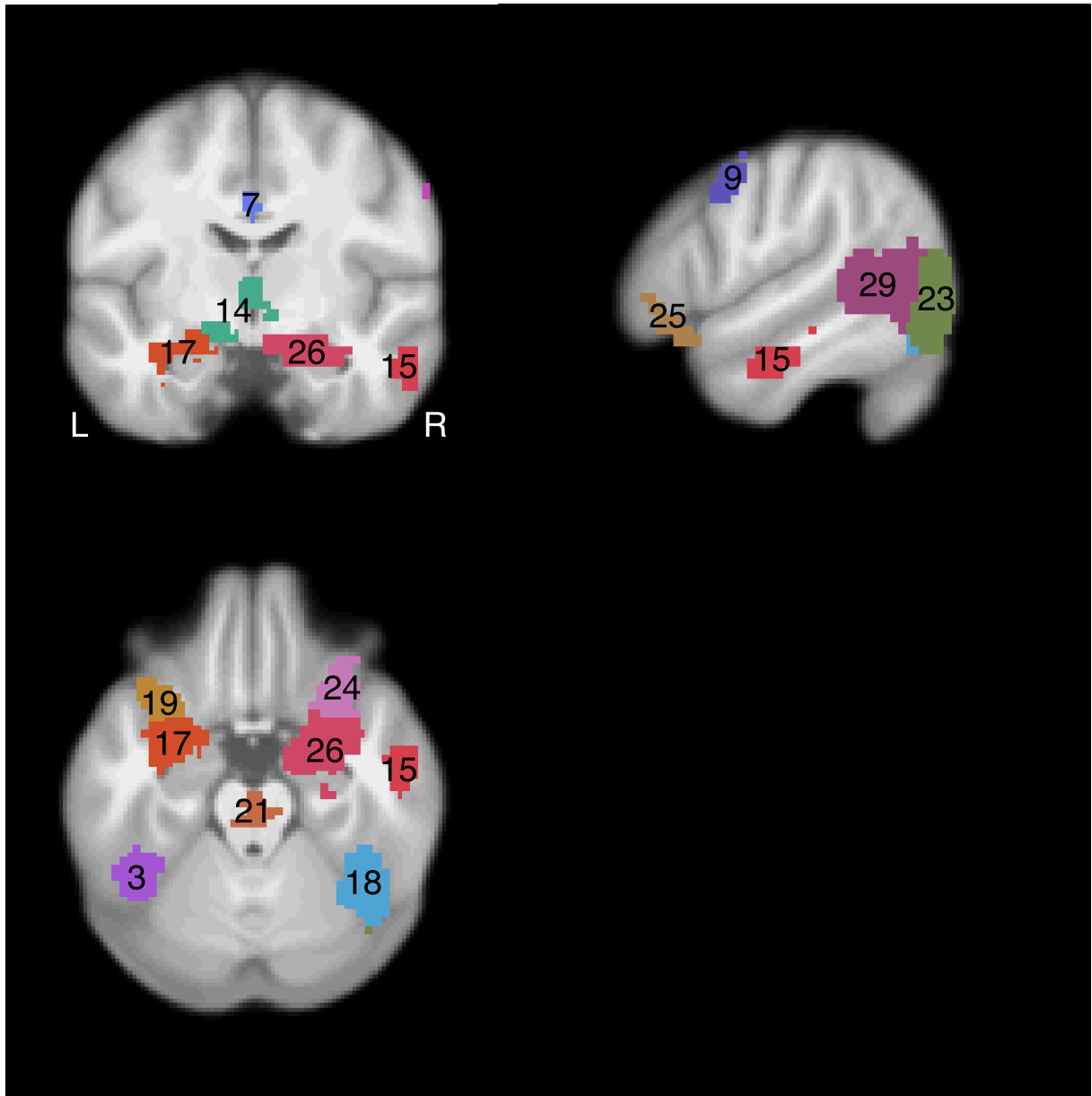


Figure S6. Result of the parcellation, where 29 spatially coherent regions of interest (ROIs) were identified. The figure depicts ROIs: 3, 7, 9, 14, 15, 17, 18, 19, 21, 23, 24, 25, 26, 29. Different colors denote different regions.

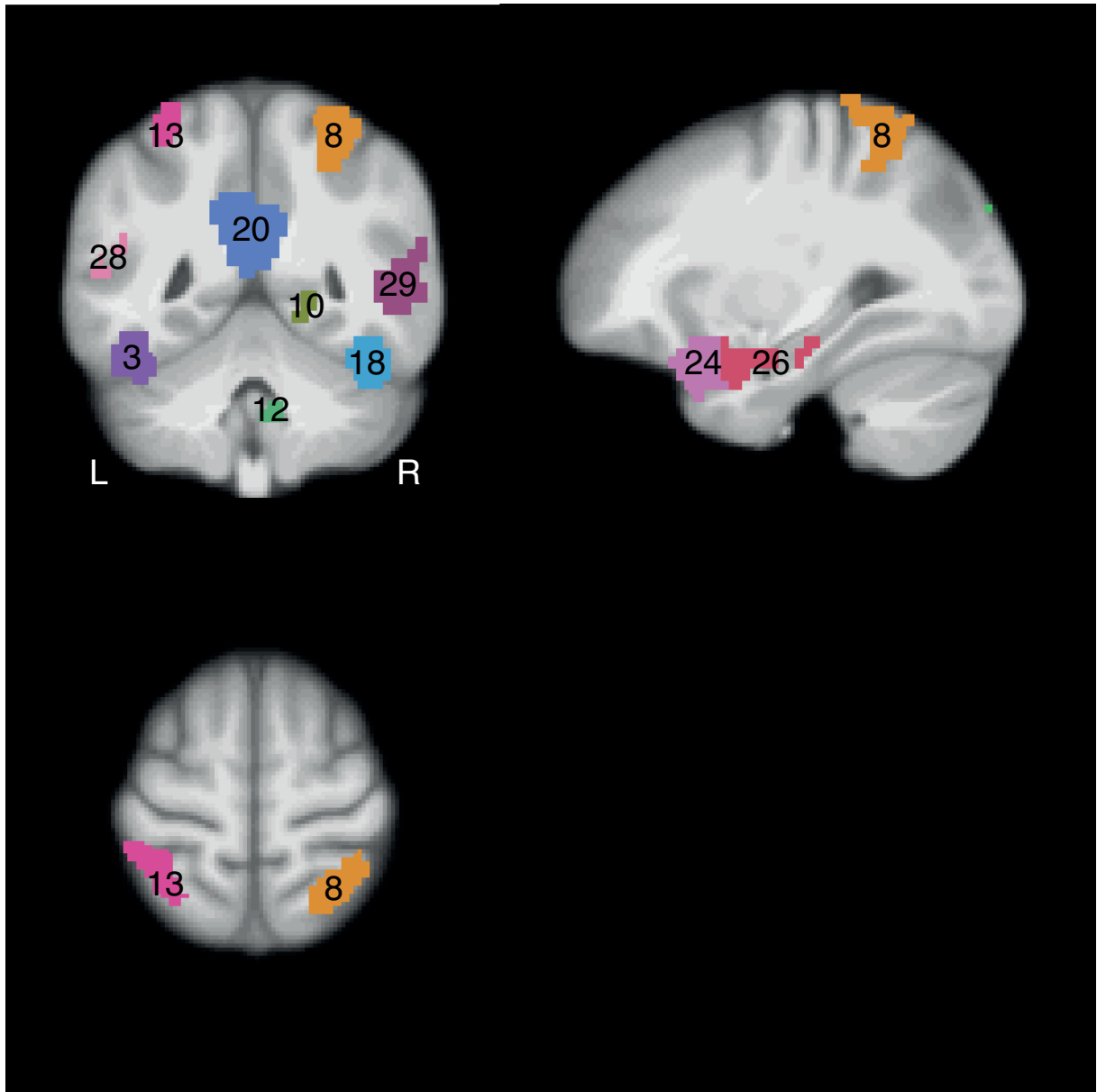


Figure S7. Result of the parcellation, where 29 spatially coherent regions of interest (ROIs) were identified. The figure depicts ROIs: 3, 8, 10, 12, 13, 18, 20, 24, 26, 28, 29. Different colors denote different regions.

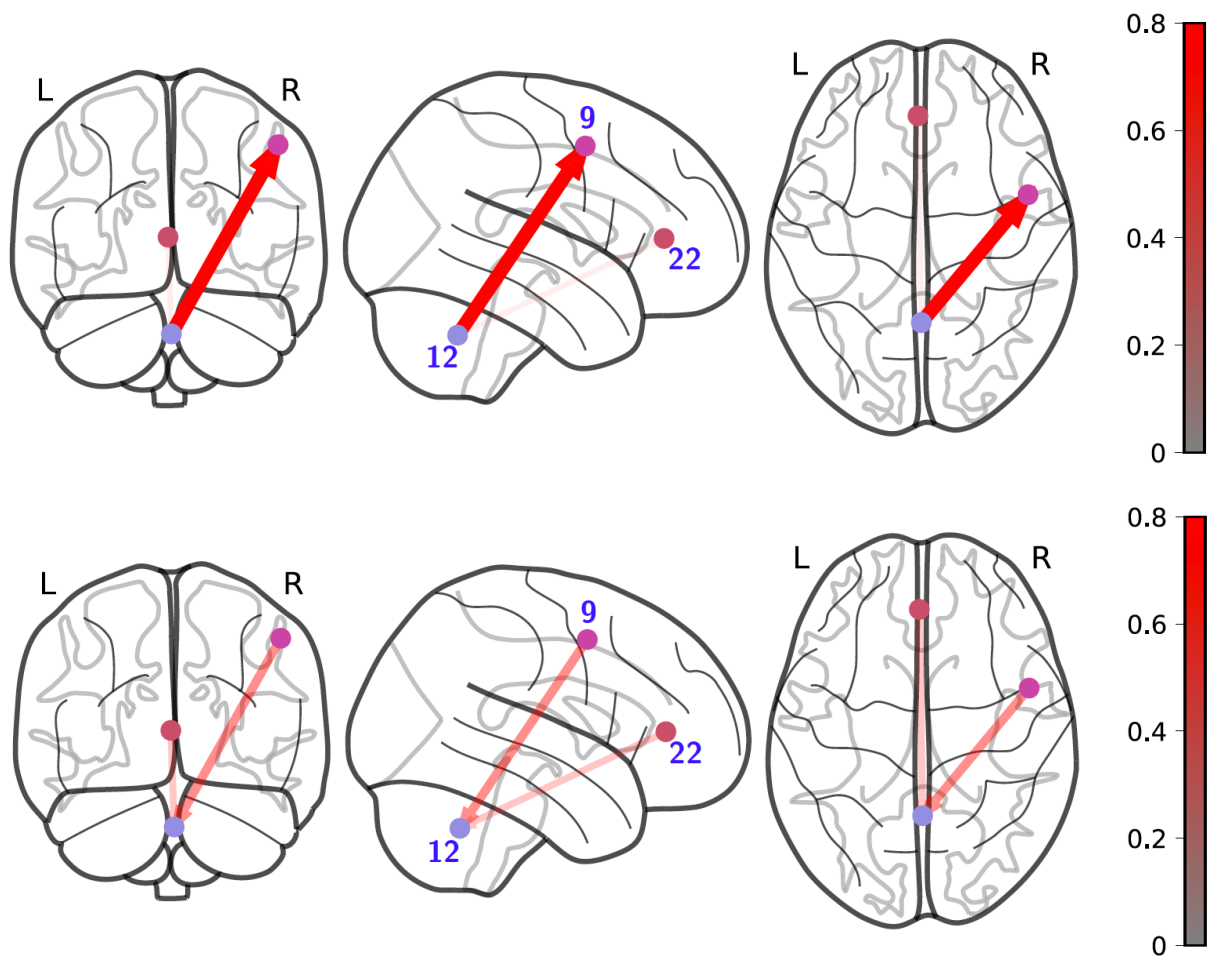


Figure S8. Bidirectional increase in the strength of cerebello-cortical connections during enhanced emotional memory encoding. The width and color of the arrows correspond to the strength of increase in connectivity in the replication sample.

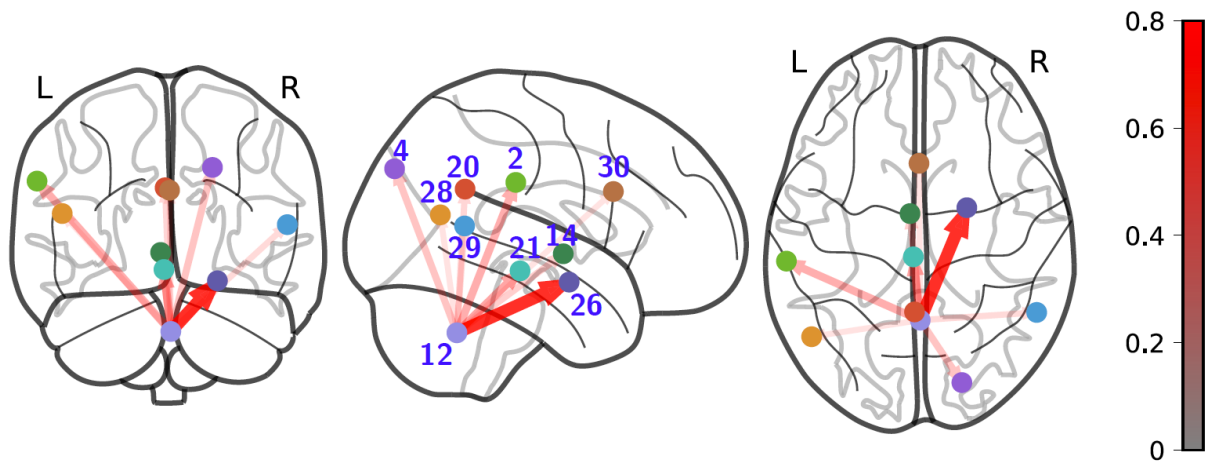


Figure S9. Increase in the strength of connections from cerebellum to cortex during enhanced emotional memory encoding. The width and color of the arrows correspond to the strength of increase in connectivity in the replication sample.

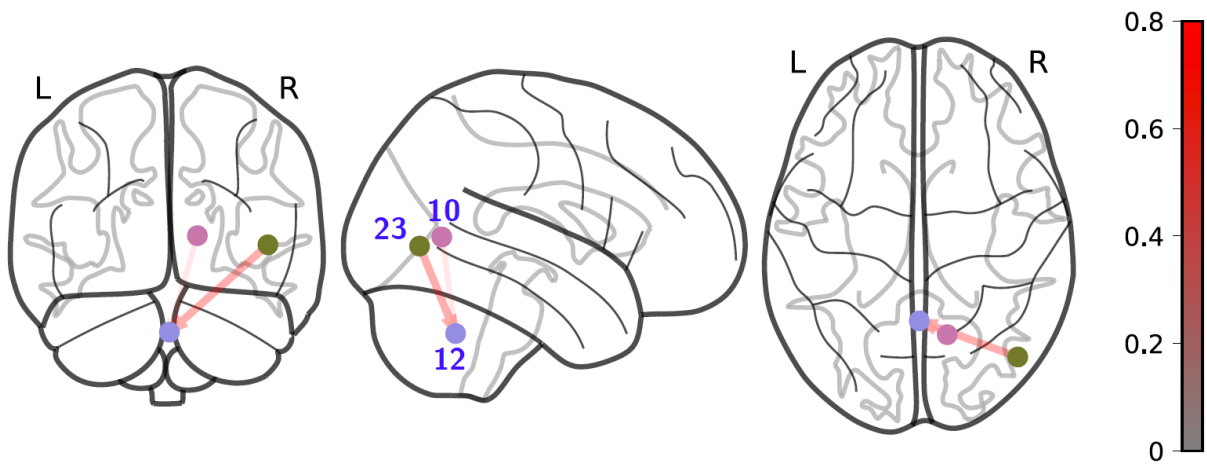


Figure S10. Increase in the strength of connections from cortex to cerebellum during enhanced emotional memory encoding. The width and color of the arrows correspond to the strength of increase in connectivity in the replication sample.